9G90-11

WEAKLY STATIONARY NOISE FILTERING of SATELLITE-ACQUIRED IMAGERY

TECHNICAL REPORT NO. 3

DECEMBER 1971

CONTRACT NO. NAS 5-21617

J. J. O. PALGEN
I. TAMCHES
E. S. DEUTSCH

prepared for
NATIONAL AERONAUTICS AND SPACE ADMINISTRATION
GODDARD SPACE FLIGHT CENTER
GREENBELT, MARYLAND

ALLIED RESEARCH ASSOCIATES, INC.
FRIENDSHIP AIRPORT · BALTIMORE, MARYLAND

WEAKLY STATIONARY NOISE FILTERING of SATELLITE-ACQUIRED IMAGERY

TECHNICAL REPORT NO. 3

DECEMBER 1971
CONTRACT NO. NAS 5-21617

J. J. O. PALGEN
I. TAMCHES
E. S. DEUTSCH

prepared for
NATIONAL AERONAUTICS AND SPACE ADMINISTRATION
GODDARD SPACE FLIGHT CENTER
GREENBELT, MARYLAND

ALLIED RESEARCH ASSOCIATES, INC.
FRIENDSHIP AIRPORT · BALTIMORE, MARYLAND

FOREWARD

The research described in this report was performed by the Geophysics and Aerospace Division of Allied Research Associates, Inc., under sponsorship of the National Aeronautics and Space Administration, Goddard Space Flight Center, Contract No. NAS 5-21617.

The authors wish to acknowledge the cooperation of Dr. A. Shulman of NASA/GSFC and Mr. N. Belknap, whose contributions were invaluable.

ABSTRACT

A type of weakly stationary noise called herringbone noise has been observed in satellite imagery. This may degrade the quality of ERTS pictorial data. The characteristics of this noise are described and a model for its simulation is developed. The model is used to degrade pictorial data for comparison with similar noise-degraded Nimbus data. Two filtering methods are defined, and evaluated. A user's application demonstration is discussed.

TABLE OF CONTENTS

LIST OF ILLUSTRATIONS

LIST OF ILLUSTRATIONS, contd.

1. INTRODUCTION

Among the more vexing problems of line-scan imaging sensors aboard earth-observing satellites is the occurrence of various types of noise that distort and degrade photometric and geometric properties of the imaged data. The herringbone noise patterns observed in the High Resolution Infrared Radiometer (HRIR) imagery from the Nimbus satellite is an example of one type of such noise. The Multispectral Scanner (MSS) on the Earth Resources Technology Satellite (ERTS) is similar to the HRIR. Thus, image cleaning through the development of effective techniques for noise removal should be considered.

This report presents the results of: (a) a definitive study of the properties of herringbone noise, including the results of a computer simulation, and (b) the initial results of a digital filtering routine which operates in the two-dimensional frequency domain.

2. BACKGROUND

Palgen (Merritt et al, 1969 and Palgen, 1970) examined the application of optical processing to diagnose and filter noise in line-scan images from Nimbus and ERTS. In the reported study, sequences of both noisy and clean Nimbus HRIR images were processed on a coherent light optical processor (Figure 1). The significance of the short parallel vertical line patterns present in the transforms was not immediately recognized. Silverman (1971), in another study of the line scan imagery from the ITOS satellite presented generated digital Fourier transforms of noisy images (Figure 2). The same pattern of two vertical lines was observed but again not understood. The author stated, "The double vertical line is difficult to explain physically. It is a function of the output display program, however, and not the processed data."

Utilizing hardwired circuits, RCA's Astroelectronics Division attempted to filter herringbone noise* from Nimbus HRIR imagery by notch-filtering the noise component in every scan line of the picture. The bandpass of the one-dimensional filter was estimated using the data from another channel in the tape recorder. The

* A discussion of the RCA filtering system is given in Palgen (1970), item 4.31, p. 16 and 17.

RCA technique improved the pictorial quality of the image for meteorlogical users. Analysis of pictorial details in the cleaned images revealed residual features which may be attributed to aliasing problems in the filter process similar to those discussed by MacGlamery (1969) in relation to white-noise filtering.

Thus, the study reported herein centers on two questions:

a) What is the nature of "herringbone" noise in the picture domain and in the frequency domain?

b) How can it be filtered digitally with minimum degradation of the image information?

3. THE NATURE OF HERRINGBONE NOISE

Herringbone noise is a weakly* stationary spatial noise which has strong local statistical autocorrelation properties. It can be viewed as an interference pattern between two or more repetitive functions such as a sinusoidal gray-level modulation of a television raster. The strong local autocorrelative property of the noise appears to manifest itself as a series of parallel shadow lines of various lengths and in different directions. These shadow lines may interfere with the visual interpretation of the pictorial information on which it is superimposed (Figure 3). The primary noise variable appears to be a sinusoidal component added to the picture along the scan direction and whose gray level amplitude of modulation, frequency and phase can be considered as random variables of unknown distributions. Studies of the satellite recording systems have shown that power consumption variations and random mechanical frictions may affect the basic frequency of the "wow" and "flutter" noise of the on-board tape recorder. This continually changing effect suggests that an amplitude modulation and/or frequency modulation concept be taken as a basis for the noise model. Amplitude modulation measurements made on a Nimbus HRIR image (Figure 3) revealed the following:

1) The basic modulating frequency (f) is 27 cycles per scan line. It is normally distributed with a variance (σ_f) of 0.5 cycles per scan line.

2) Quantitative modulation measurements obtained with an optical scanner

* A weakly stationary random process is one whose expectations (mean, variance, correlation, etc.) are slowly varying with translation in time. A test of the hypothesis that the data sample is weakly stationary can be found in Enochson and Otnes, 1968.

indicated a gray level amplitude modulation of approximately 20%.

3) The presence of variable horizontal bands of strong local spatial correlation whose widths are quasi-binomially distributed.

To obtain a better understanding of the nature of the herringbone noise, two different approaches using a computer for noise simulation were taken. Both used the basic parameters listed above together with an intuitive concept of the noise structure.

In the first simulation approach, a routine was developed which was essentially a continuous frequency modulation model where the frequency was varied at each pixel by a pseudo-random number generation routine. While it generated an image of pseudo-herringbone (Figure 4), it did not prove promising by visual inspection, and therefore was discarded.

In the second simulation approach the frequency was held constant along a scan line and modified with each new scan line. The noise simulation subroutine was based on a sinusoidal function with its frequency uniformly distributed between 26.5 and 27.5 cycles per scan line. The assumption of constant frequency yields a considerable saving in computer time. Gray-level amplitude modulation was held at 20%. Two examples of pseudo-herringbone noise images generated by this approach are presented in Figure 5. These patterns favorably simulate the noise. Visual analysis of the data on two adjacent raster lines explains the appearance of the typical parallel gray-level regions oriented at a given angle. Figure 6 presents a schematic local representation of the patterns.

The same pattern relationships can be expressed in the two-dimensional Fourier domain. Referring to Figure 6, it is clear that:

1) $b = a \sin \theta$

Thus, using a sinusoidal gray level modulation of the scan line, the representation of the gray level bands in the two-dimensional Fourier domain consists of energy concentration points (Figure 7).

These energy concentrations are located a distance d from the transform's center and at an angle φ to the horizontal frequency line.

The distance d and the angle φ are given by:

2) $d = \frac{1}{b} = \frac{1}{a \sin \theta}$

and

3) $\varphi = \theta - 90^{o}$

Taking into account that bands can take every possible orientation, it is expected that the visual bands considered to be the herringbone noise in the pictorial domain have most of their energy randomly concentrated along two parallel lines in the Fourier domain. The distance between the energy lines is $2/a$ and those lines should be centrally located perpendicular to the horizontal frequency axis (Figure 8). The digital two-dimensional Fourier transform of the pseudo-herringbone noise image is, in fact, distributed along the two predicted parallel lines (Figure 9). A typical noise energy distribution along spectral line (A-A') is shown in Figure 10.

Experiments have shown that frequency-modulating the fundamental noise frequency in the pictorial domain causes a broadening of the spectral lines about their corresponding center in the Fourier domain. Also, data truncation, such as that occurring during sensor saturation, produced harmonic vertical parallel lines in the Fourier domain. Both effects lower the obtainable signal-to-noise ratio of the picture after filtering.

Further confirmation of the validity of the computer-simulation of herringbone noise is obtained from visual examination of a Nimbus satellite subpicture* and its digital Fourier transform. The parallel herringbone noise lines are easily identified in the Fourier domain, while the visual noise can hardly be noticed in the picture (Figures 11 and 12)**.

4. HERRINGBONE NOISE FILTERS

Filtering the herringbone noise from affected line scan imagery is a complex problem, especially since the frequency of the noise is often close or identical to the

---

* A subpicture is defined as a dimensional-limited (N x N) subset of the picture matrix, generally kept at 64 x 64 elements due to computer memory limitation.

** This pattern of parallel vertical lines is analogous to the optical transforms prepared by Palgen (1970) and the digital transforms presented by Silverman (1971) but not understood in either case.

frequency of parts of the pictorial information. Therefore, it is necessary to devise a technique to enhance the pictorial signal-to-noise ratio.

4.1 One-Dimensional Filtering - RCA

Considering herringbone noise to be generated by a one dimensional random process, RCA adopted a one dimensional filtering approach to remove this noise from Nimbus imagery. This approach, where the notched frequency-filter was defined by a one-dimensional Fourier analysis, improved the overall visual appearance with some improvement in the depiction of large meteorological features and a little improvement in small-size features. Some features were found to be added or subtracted in a manner analogous to the mathematical "aliasing" phenomena described by MacGlamery (1969). A cumulative one-dimensional Fourier transform was obtained for Figure 14b by summing the transforms of the 64 horizontal scan lines, as shown in Figure 16a. Noise and signal share the same bands in the one-dimensional transform and they cannot be separated without affecting the energy of the signal in these bands.

4.2 Two-Dimensional Filtering - ARA

During the study and review of the background experiments and literature of quasi-stationary noise filtering, optical filtering concepts and optical-digital filtering techniques were compared.

The two-dimensional filtering approach used in this study makes extensive use of the model understanding gained through simulation of the nature of herringbone noise. Initial tests have been accomplished using simulated noise superimposed on an Apollo 9 (S065) photograph of the Salton Sea area.

Figures 13 and 14 present the scanned and digitized test imagery in clean and noisy forms respectively. A subpicture of 64 x 64 pixels is shown extracted

from each one. The Fourier transforms of Figures 13b and 14b are shown in Figures 15a and 15c respectively. In the Fourier transform, the primary energy of the undegraded subpicture is at the center of the transform (Figure 15a). Noise energy is distributed along vertical parallel lines, symmetrically located about the center (Figure 15b).

The two-dimensional digital filtering routine for the herringbone noise presented here operates in the Fourier domain in a manner which is analogous to coherent optical filtering. In the tests, the noise distribution in the spatial frequency domain was initially estimated from a noisy subpicture area having a low gray level variance. The one-dimensional cumulative Fourier transform of such an area was obtained and the noise energy found to be strongly localized to a narrow band in the one-dimensional case (similar to Figure 16). Therefore, the location of this band was easily estimated from the absolute magnitude of the slope of the cumulative one-dimensional Fourier transform curve. On this basis, self-adapting binary energy blocking filters were applied in the two-dimensional Fourier domain (Figure 18). The indicated positions show the areas of energy blocked in each step in the test filtering sequence. At each step, a reconstructed image is obtained from the filtered transform. A useful diagnostic tool was developed during the testing, utilizing outputs of the noise residuals at each step in the filtering sequence. Figure 17a-e presents the sequence from the original clean image to the filtered image showing (in Figure 17f-i) the appropriate residuals at each step.

The signal-to-noise ratio, at each step, is defined as the ratio of the cumulative signal power to the cumulative noise power obtained from the Fourier transforms of the respective filtered pictures. At step four, in which the entire energy in the frequency band is filtered (one-dimensional - RCA), the signal-to-noise ratio is less than step three. This indicates that one-dimensional band-stop filtering is inferior to the band-selective binary line filtering used in two-dimensional filtering.

As an ultimate test of the effectiveness of two-dimensional filtering for the elimination of herringbone noise with periodic frequencies close to the information frequencies, 512 x 512 pixel images of a sinusoidal bar pattern with a frequency of 27 cycles per frame were prepared and a herringbone superposed. The same 27-cycle generating function described in Section 3 was used. Thus, the pictorial

information and the noise share the same one-dimensional frequency band (Figure 20). The filtered image (Figure 20d) is very nearly the same as the original (Figure 20a)*. The residuals shown in Figure 20e are hardly noticeable.

5. USER APPLICATION DEMONSTRATION

The effectiveness of any image-filtering routine depends on its demonstrated potential to extract pictorial information from noisy images. Studies reported thus far have emphasized development and testing of filtering routines. In the following, a brief example of the enhancement potential of the herringbone filter for either visual or machine-assisted image information extraction is discussed.

5.1 Visual Interpretation

Visual image interpretation is partly dependent on the identification of shapes (edge detection), tones, and texture. The influence of the filter on these image parameters is therefore important. Density cross sections over selected areas of an image can improve some user-oriented information on how a filtering routine affects edge detection. For illustrative purposes, some of the images shown in Section 4 (Figure 17) are presented again, with the indicated locations of the selected density cross sections, (see Figure 21). The scene is taken from an agricultural area, and identifies crop tonal patterns, etc. The density cross sections identified as A-A', B-B' and C-C' in Figure 21 present, (a) the clean image; (b) the noisy image, and (c) the filtered image. Note that the predominant effect of the herringbone noise on the cross section is in the accentuation and lateral displacement of the gray scale peaks and valleys existing in the original clean image. After filtering, the artificial peaks and valleys return to their original locations and the overall density levels return to the average levels in the clean image. The potential for correct edge identification and thereby visual shape and texture extraction has been reinstated.

---

* The "edge" effects relate to the border discontinuities on the periodic characteristics of the Fourier operations on the 64 x 64 array.

5.2 Machine-Assisted Interpretation - Multispectral Discrimination Techniques

The multispectral discrimination techniques developed by the Laboratory for Agricultural Remote Sensing (LARS) at Purdue University operate, in part, by fitting experimental multispectral data statistics to an assigned joint probability density surface in an n-dimensional vector space for each class of feature to be discriminated (Landgrebe, 1968). Effective operation of the technique is therefore limited by the noise affecting the joint probability distributions (the statistical spread). In application, the noise-generating function may be independent for each spectral band. Due to herringbone noise, a serious increase in statistical spread may be expected. To provide a brief test of the influence of the filter on statistical density distributions, histograms were prepared for clean, noisy and filtered images (Figure 22). The noise histograms of Figure 22b show the distribution is broadened, and of significantly different shape than in Figure 22a. It is speculated that such distribution modifications would introduce a serious increase in discrimination errors by introducing undefined features into each of the three or four channels of data which are modified differently by the noise. The filtered histogram, Figure 22c, shows a marked return to the overall shape of the clean histogram. Intuitively, it appears that the LARS discrimination capability would be reinstated with the filtered statistics. Only future tests will confirm this statement.

6. CONCLUSIONS AND RECOMMENDATIONS

This study had as its basic objectives: (a) definition of the properties of the herringbone noise pattern often found in line-scan imagery from various spaceborne sensors, and (b) development of routines to filter herringbone noise using digital techniques.

6.1 Conclusions

Herringbone noise is a two-dimensional noise pattern, generated by a one-dimensional process which can be approximated by a sinusoidal amplitude-modulated

signal with random frequency modulation from scan line to scan line. Computer simulations employing this relatively simple model produce a noise pattern closely resembling that observed in real imagery.

The study of the two-dimensional Fourier properties of herringbone noise reveals that the noise energy clusters in two parallel lines perpendicular to the horizontal frequency axis. Binary blocking filters introduced into the Fourier domain provide improved images which appear superior to those obtained with a comparable one-dimensional scan line filter introducing a bandpass notch derived from a one-dimensional Fourier analysis. The two-dimensional frequency filter advantage resides in the fact that the noise is less coherent from line-to-line than the pictorial data. The two-dimensional frequency domain filter appears effective even in the extreme case when the picture and the noise share essentially the same bands in the two-dimensional frequency domain.

Evaluation of the influence of the filtering routine on visual and machine-aided information extraction are in progress. Preliminary results indicate a significant improvement on the potential for useful feature extraction in the filtered image. The results appear most relevant to machine-assisted feature extraction techniques such as the Purdue LARS technique in which the statistical distribution of the pictorial densities in every multispectral band is very important.

6.2 Recommendations

The study has shown the need for image noise filtering to enhance the uses of satellite images in manual and machine-aided multispectral discrimination applications. Two-dimensional filtering using Fourier transform techniques is feasible and more effective than one-dimensional techniques for filtering weakly stationary noise of the herringbone type.

The following specific recommendations are made:

1) Image filtering tests should continue, culminating in a comparison using the LARS routines operating on clean and noisy images.
2) Positional definition of the binary block filter should be automated by taking advantage of the shape of the cumulative energy curve in the

Fourier domain.

3) The effectiveness of nonbinary and self-adaptive filters should be evaluated.
4) An operational image-processing system should permit Fourier processing of the 512 x 512 pixel arrays.
5) Image mosaicing routines should be developed to permit computer recompositing of subarrays into larger arrays after filtering.

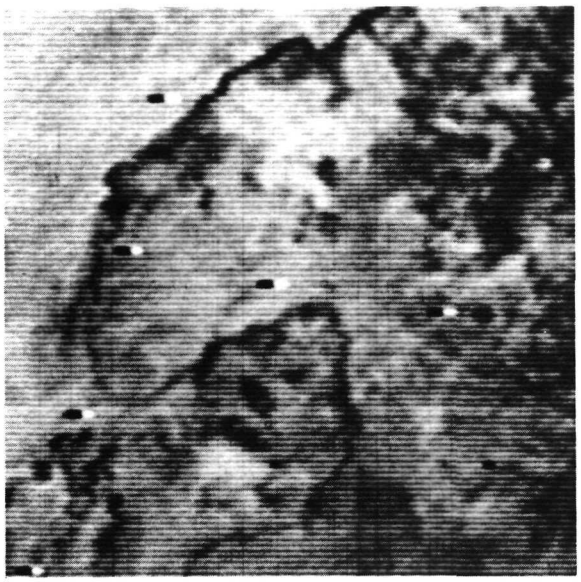

a. Normal HRIR image.

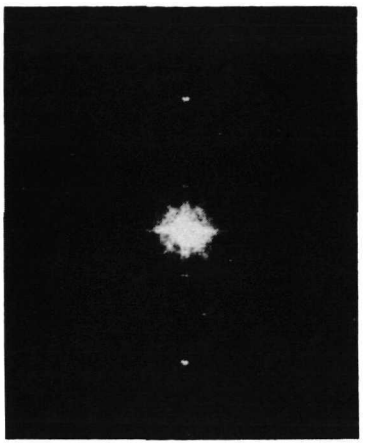

b. Optical Fourier transform of image (Fig. 1a) HRIR

Figure 1 Example of Nimbus 3 HRIR image (Sudan, Egypt - Nile Valley) degraded with various degrees of herringbone noise and their respective optical Fourier transforms.

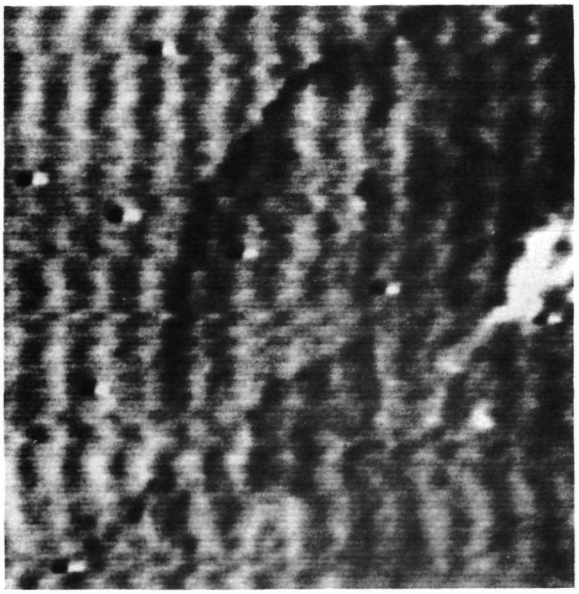

c. Typical degraded image

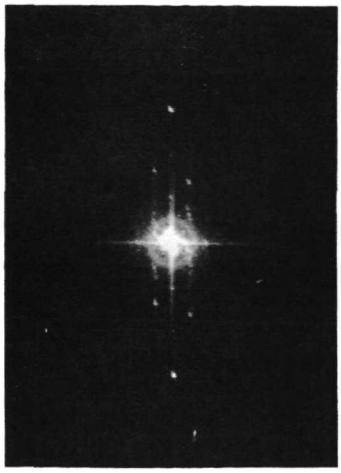

d. Optical Fourier transform of degraded image in Figure 1c.

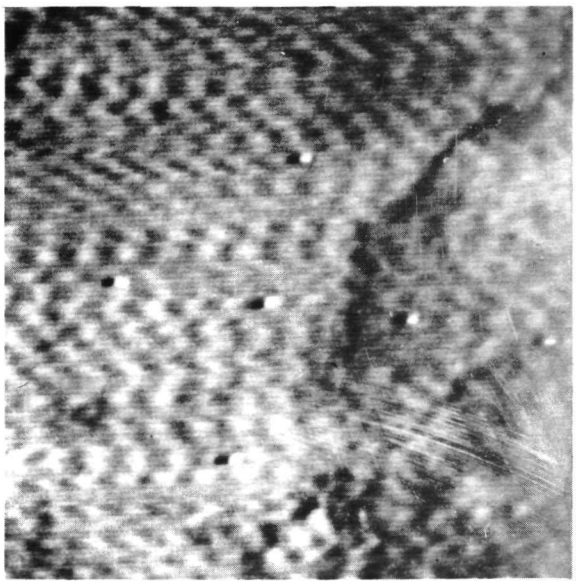

e. Typical degraded image

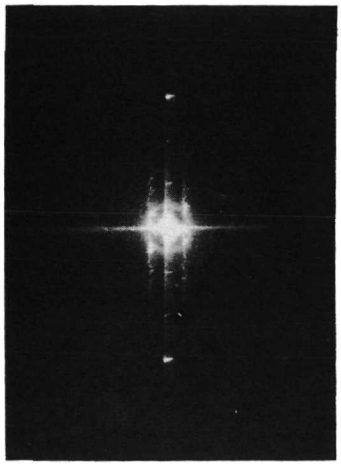

f. Optical Fourier transform of degraded image in Figure 1e

Figure 1 contd.

The optical transforms were generated in cooperation with A. Shulman, NASA/GSFC.

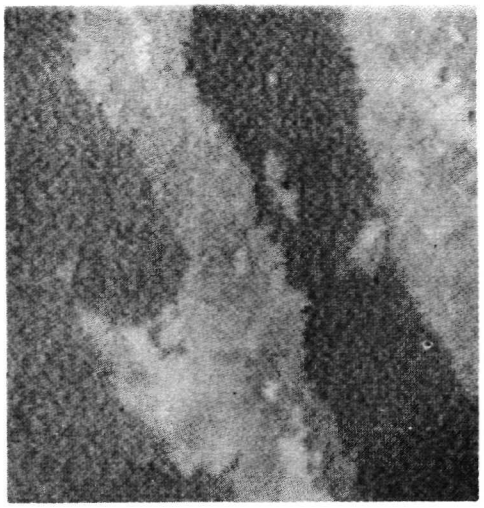

a. Unfiltered image (from ITOS satellite)

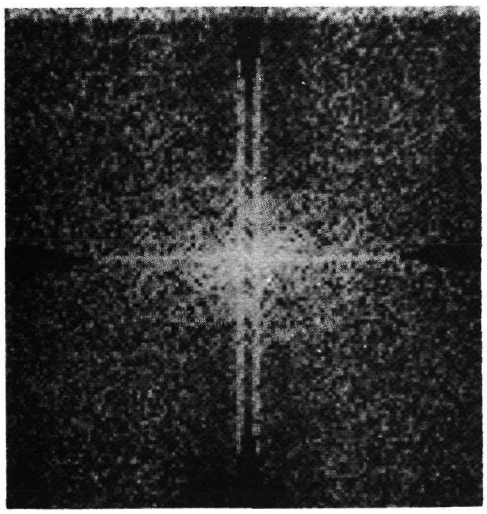

b. Digital display of the log of the magnitude of the Fourier transform of Figure 2a.

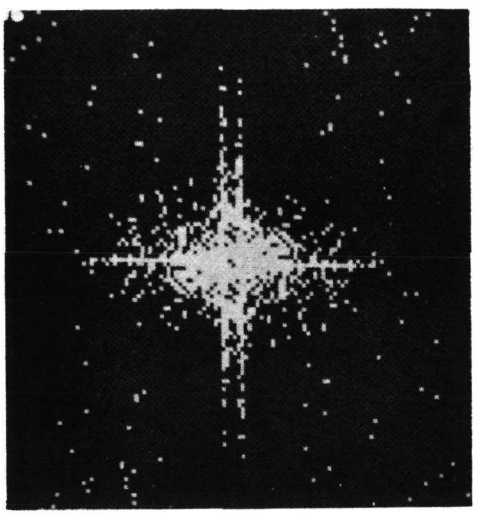

c. Digital display of the quantized Fourier transform magnitude of Figure 2a.

Figure 2 An ITOS image and its digital Fourier transform (after Silverman, 1971)

Figure 3 Example of Nimbus 3 HRIR image (Red Sea), with added "herring-bone" artifacts (related to the on-board tape recorder). Courtesy NADUC, NASA/GSFC; August 1969).

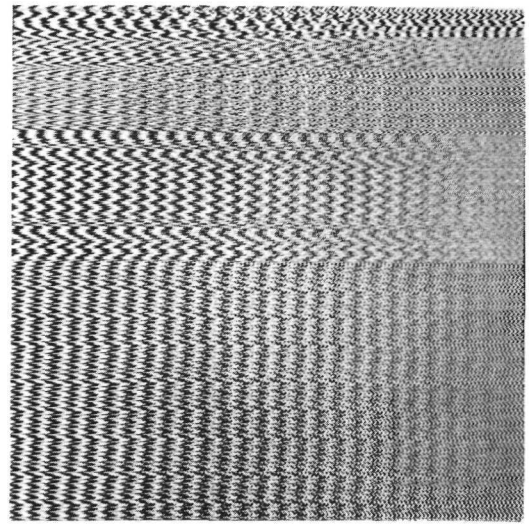

Figure 4 Computer-generated herringbone noise pattern based on the first noise model and its statistics obtained from Figure 3 (see p. 2).

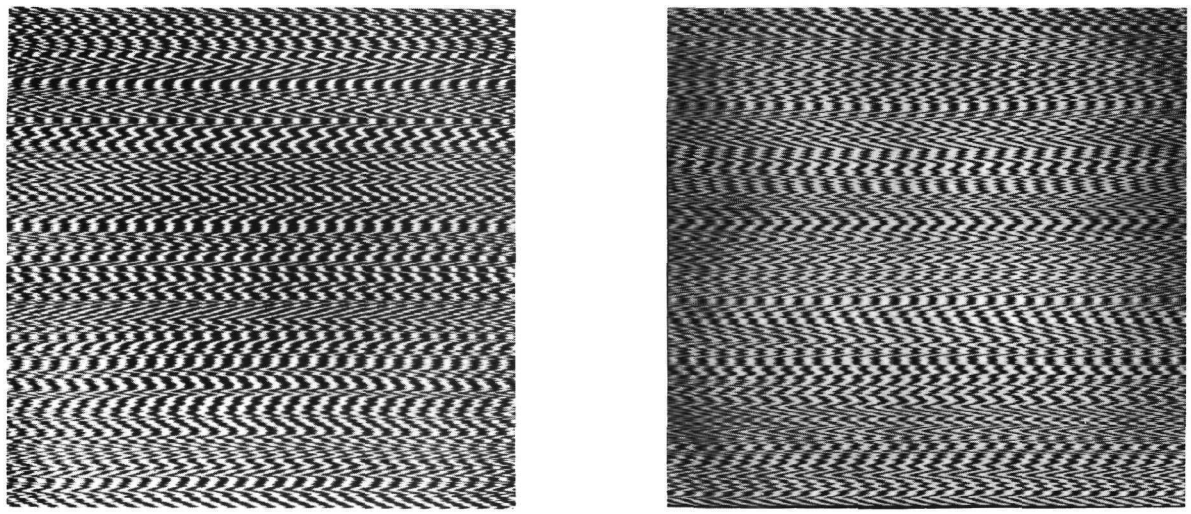

Figure 5 Computer-generated herringbone noise pattern based on the second noise model. The pictures above have the same noise model, but were generated using different pseudo-random sequences.

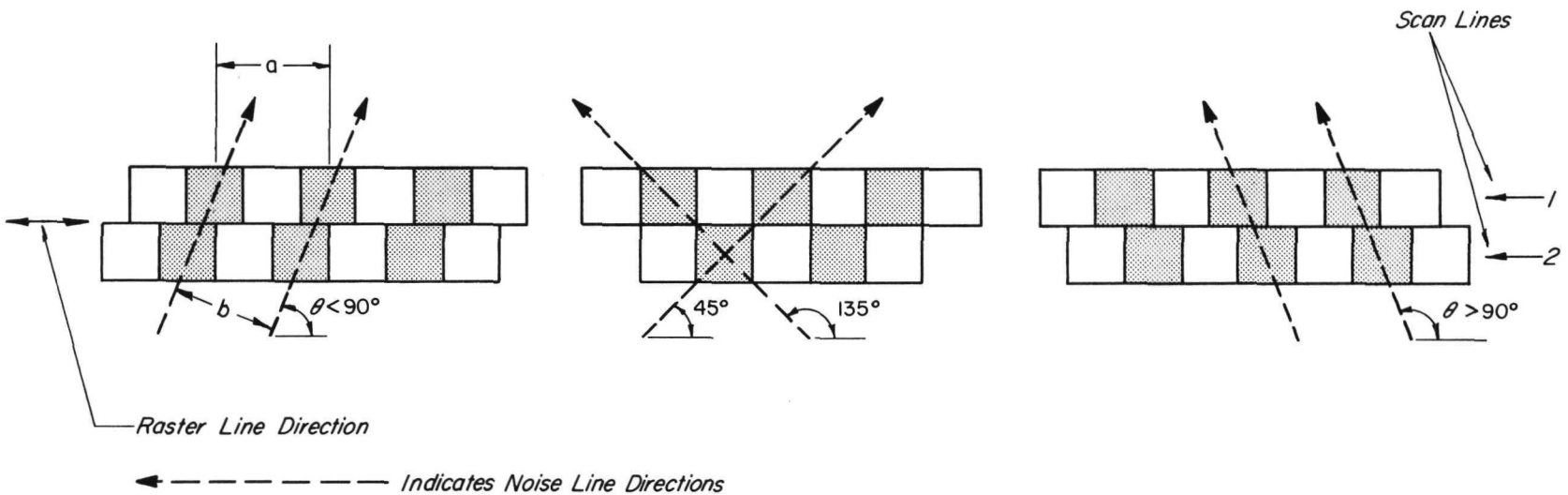

Figure 6 Possible spatial arrangement of the peaks of the noise along two adjacent raster lines.

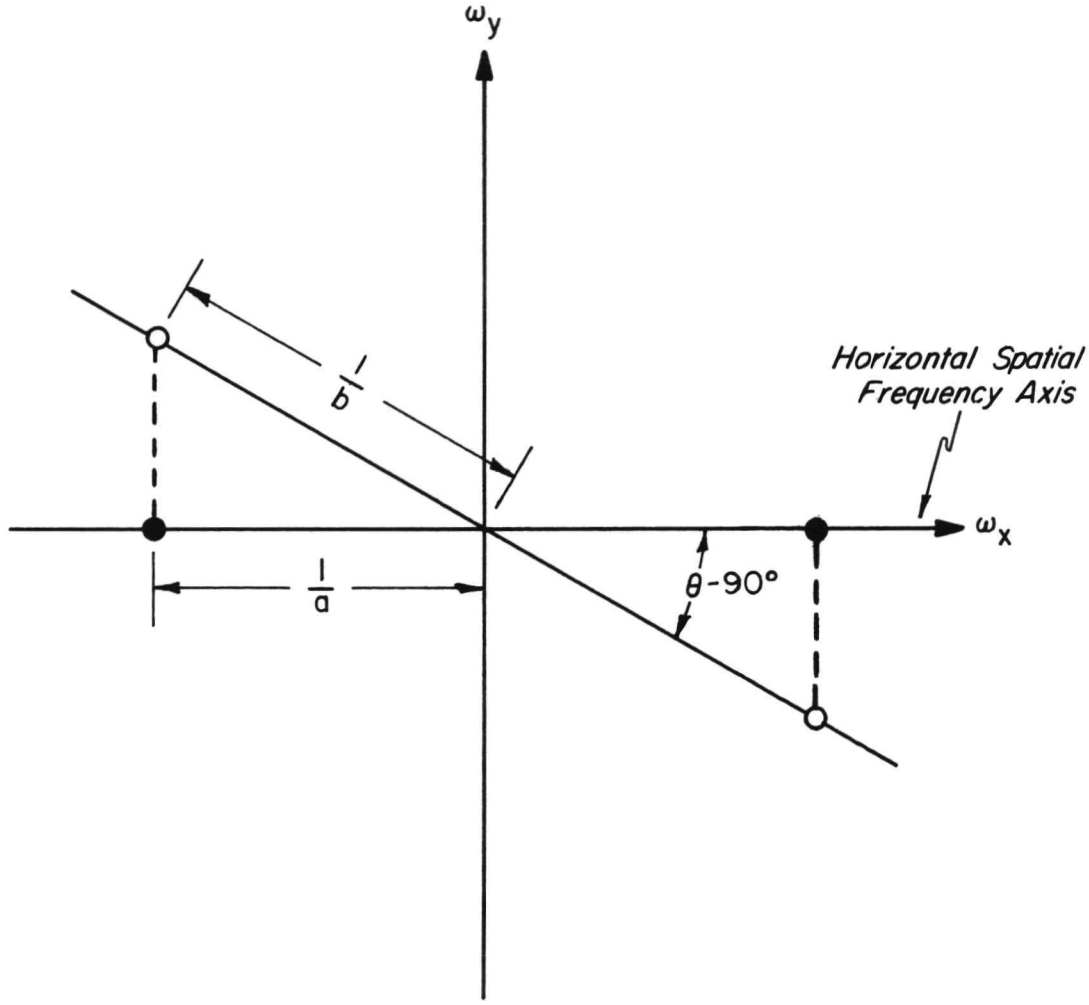

- ● *Vertical Bars Generated by Sinusoids of Period "a" and Coherent from Line to Line*
- ○ *Slanted Bars Generated by Sinusoids of Period "a" and Incoherent from Line to Line by Angle θ*

Figure 7 Two-dimensional Fourier transform representations of sinusoidal bar patterns.

7830

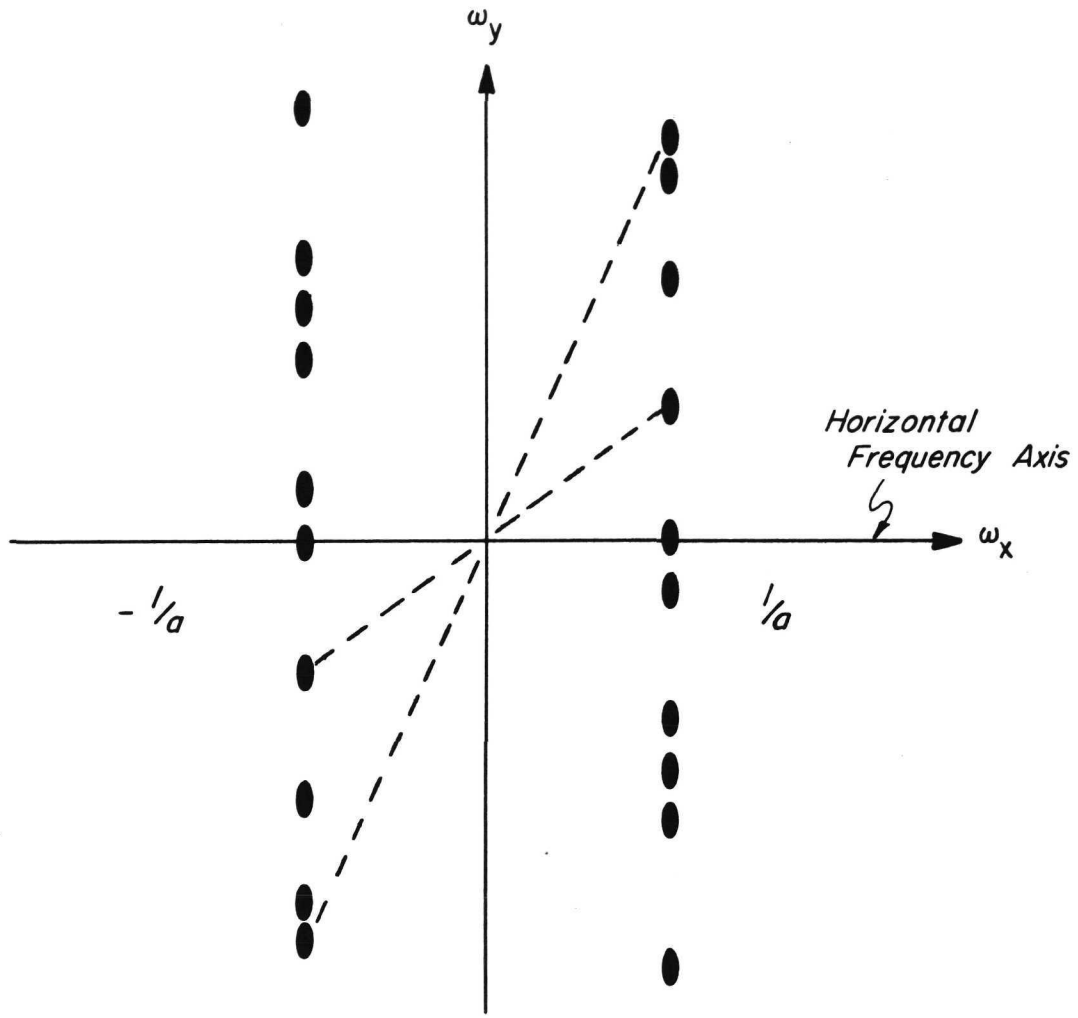

7829

Figure 8 Predicted locus of the energy concentration of herringbone noise, in the frequency domain.

a. Herringbone noise pattern.

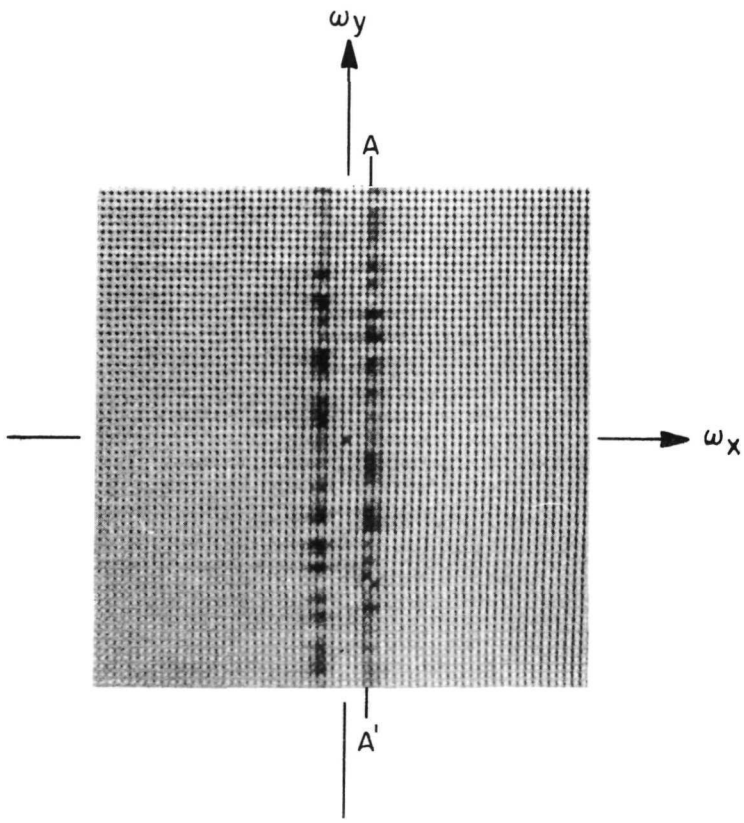

b. Spatial frequency representation of the noise shown in Figure 9a.

Figure 9 Herringbone noise pattern and its spatial frequency representation.

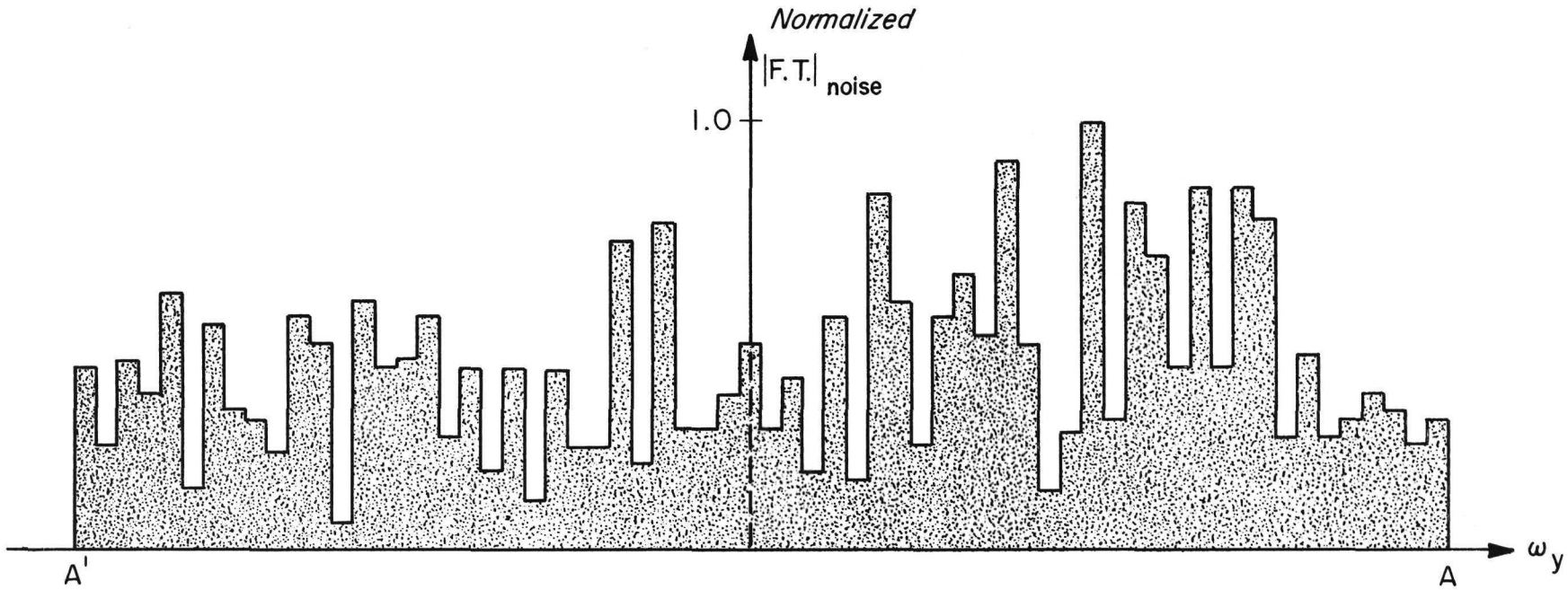

Figure 10 A typical energy distribution of herringbone noise along its prescribed locus in the spatial frequency domain, based on the example in Figure 9b.

Figure 11 Nimbus 3 IDCS image (Greenland and Iceland). Orbit 16, 15 April 1969. Arrow indicates location of a 64 x 64 sub-picture utilized in Figure 12. The presence of herringbone noise at subliminal level is indicated by the typical Fourier transform signature shown in Figure 12. b.

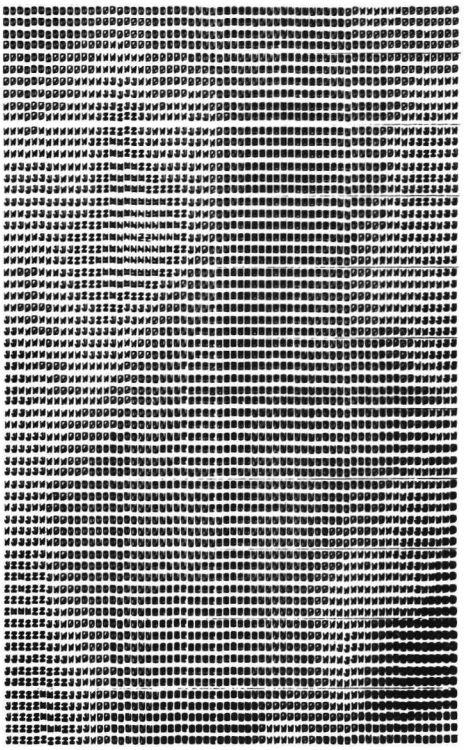

a. Subpicture window (64 x 64) obtained from digitized Nimbus 3 IDCS imagery.

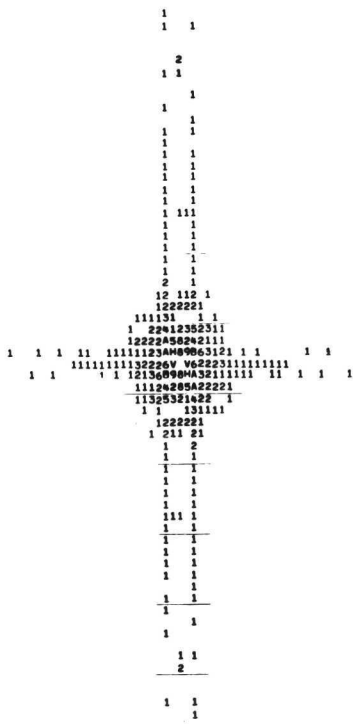

b. Digital Fourier transform of the subpicture shown in (a). The observed parallel align pattern is the "signature" of the herringbone noise, in the frequency domain.

Figure 12 Computer detection of herringbone noise in the digital Fourier transform domain.

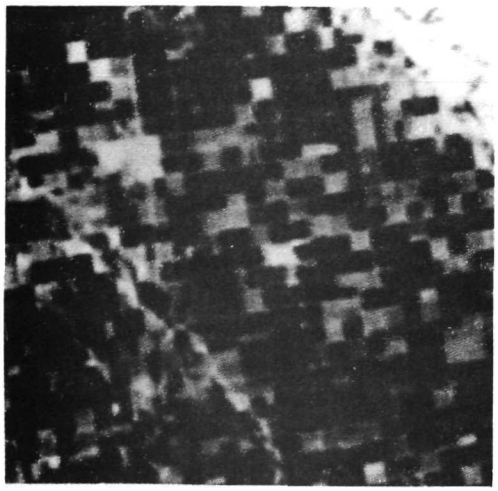

a. Main input picture

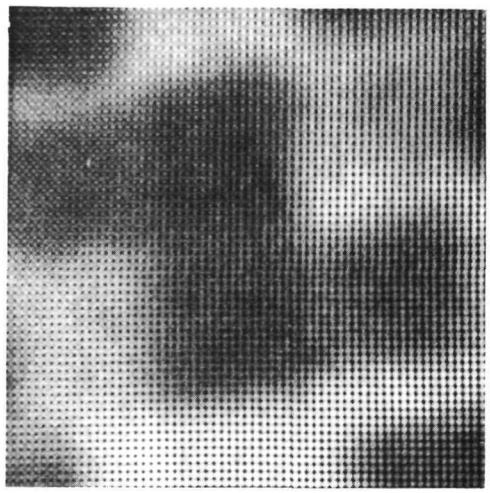

b. Input subpicture

Figure 13 Scanned and digitized test imagery in its undegraded form.

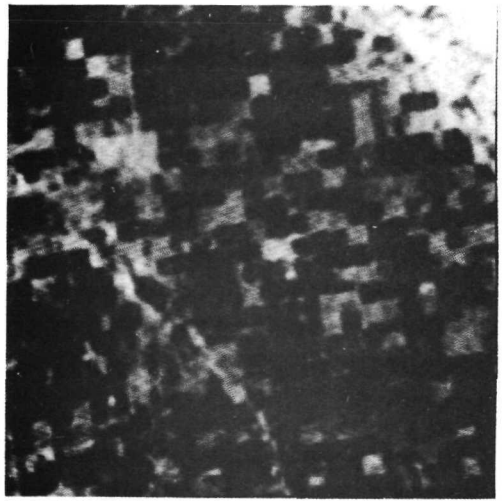

a. Main picture with herringbone noise added.

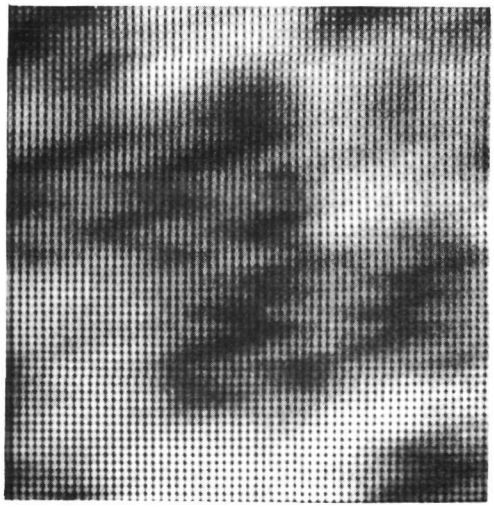

b. Subpicture with herringbone noise added.

Figure 14 Scanned and digitized test imagery with Herringbonc noise added.

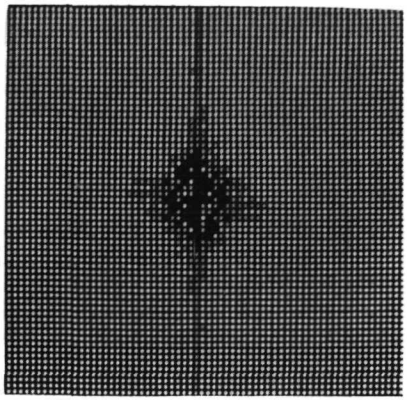

a. Fourier transform of the input subpicture shown in Figure 13. b.

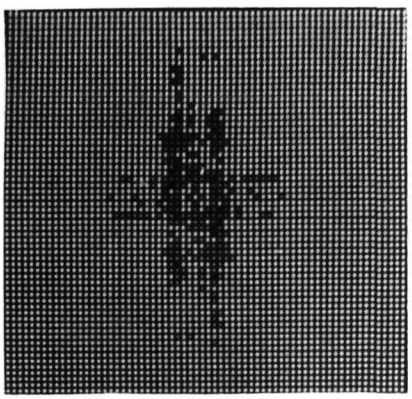

b. Fourier transform of the herringbone noise.

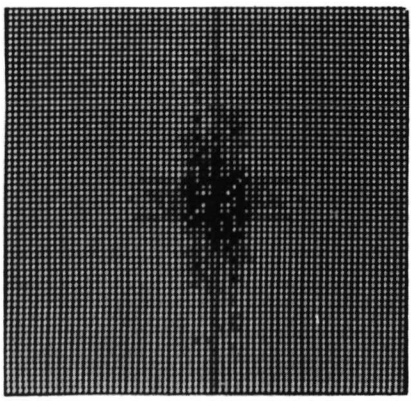

c. Fourier transform of the noisy subpicture shown in Figure 14. b.

Figure 15 Spatial frequency representations.

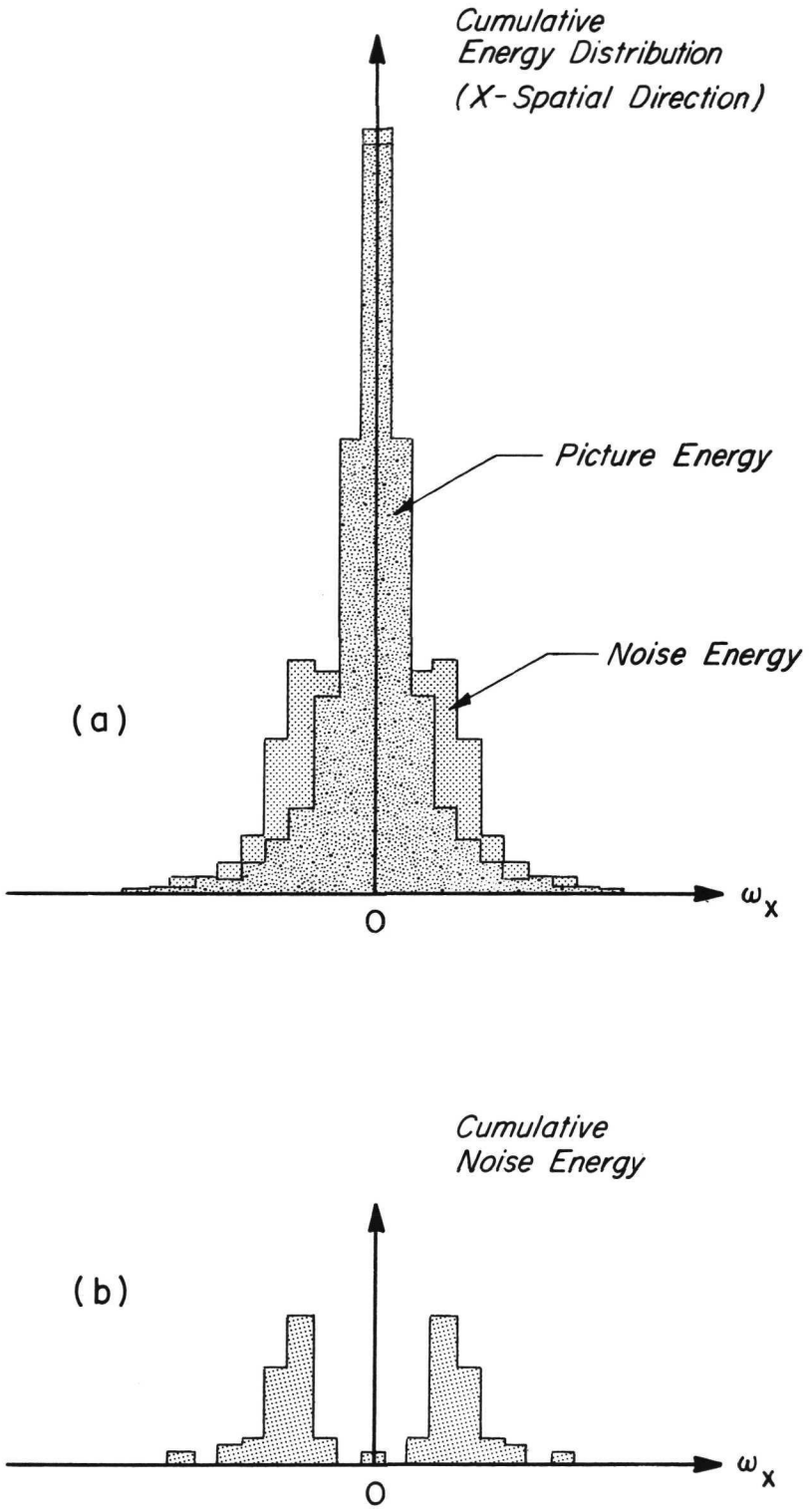

Figure 16 Cumulative one-dimensional spatial representation of the Fourier Transform of the subpicture shown in Figure 14b.

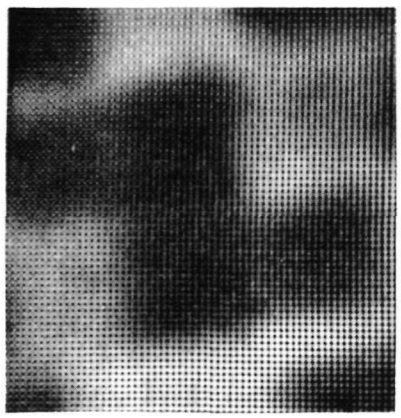

a. Input picture subset (shown for comparison).

b. Picture subset with herringbone noise added before filtering.

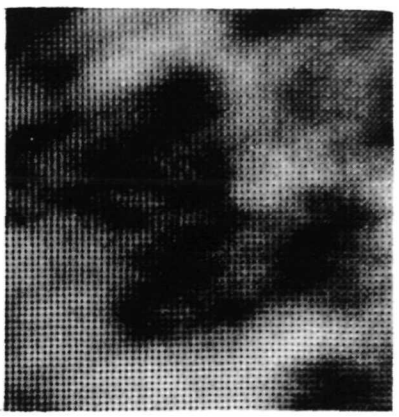

c. Picture subset with herringbone noise added, after passing through filter step 1.

d. Picture subset with herringbone noise added, after passing through filter step 2.

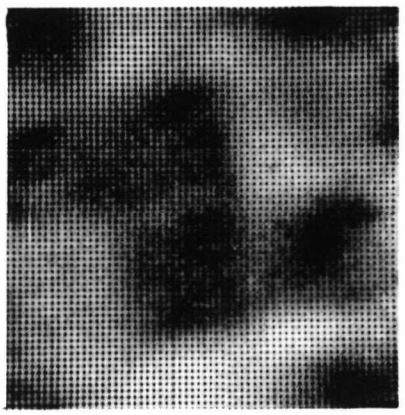

e. Picture subset with herringbone noise added, after passing through filter step 3.

Figure 17 Filtering results.

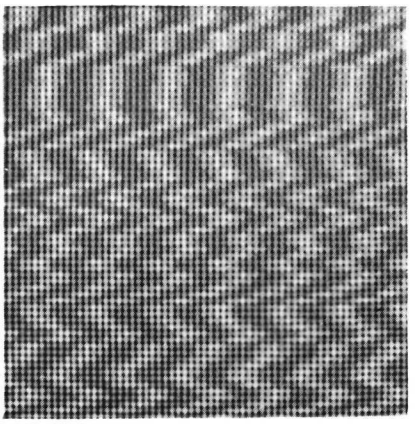

f. Original noise residues before filtering, i.e. Fig. 17. b. minus Fig. 17. a.

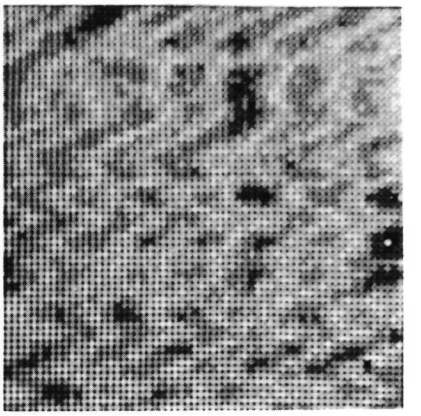

g. Noise residues after passing through filter step 1, i.e., Fig. 17. c. minus Fig. 17. a.

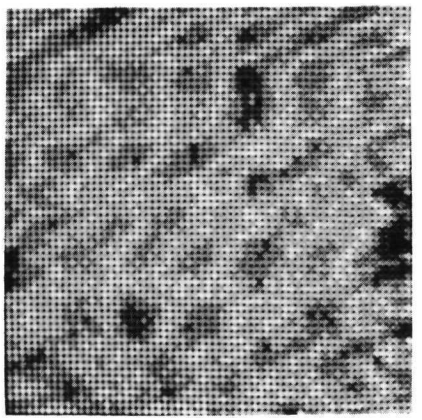

h. Noise residues after passing through filter step 2, i.e. Fig. 17. d. minus Fig. 17. a.

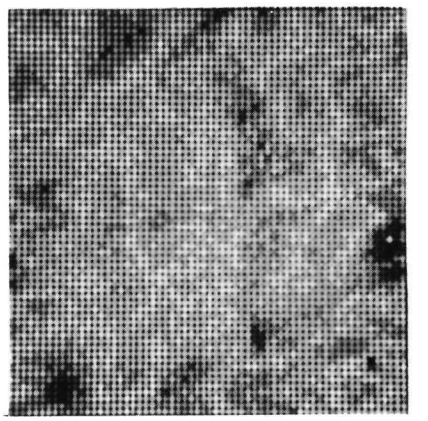

i. Noise residues after passing through filter step 3 i.e. Fig. 17. e. minus Fig. 17. a.

Figure 17 (cont'd)

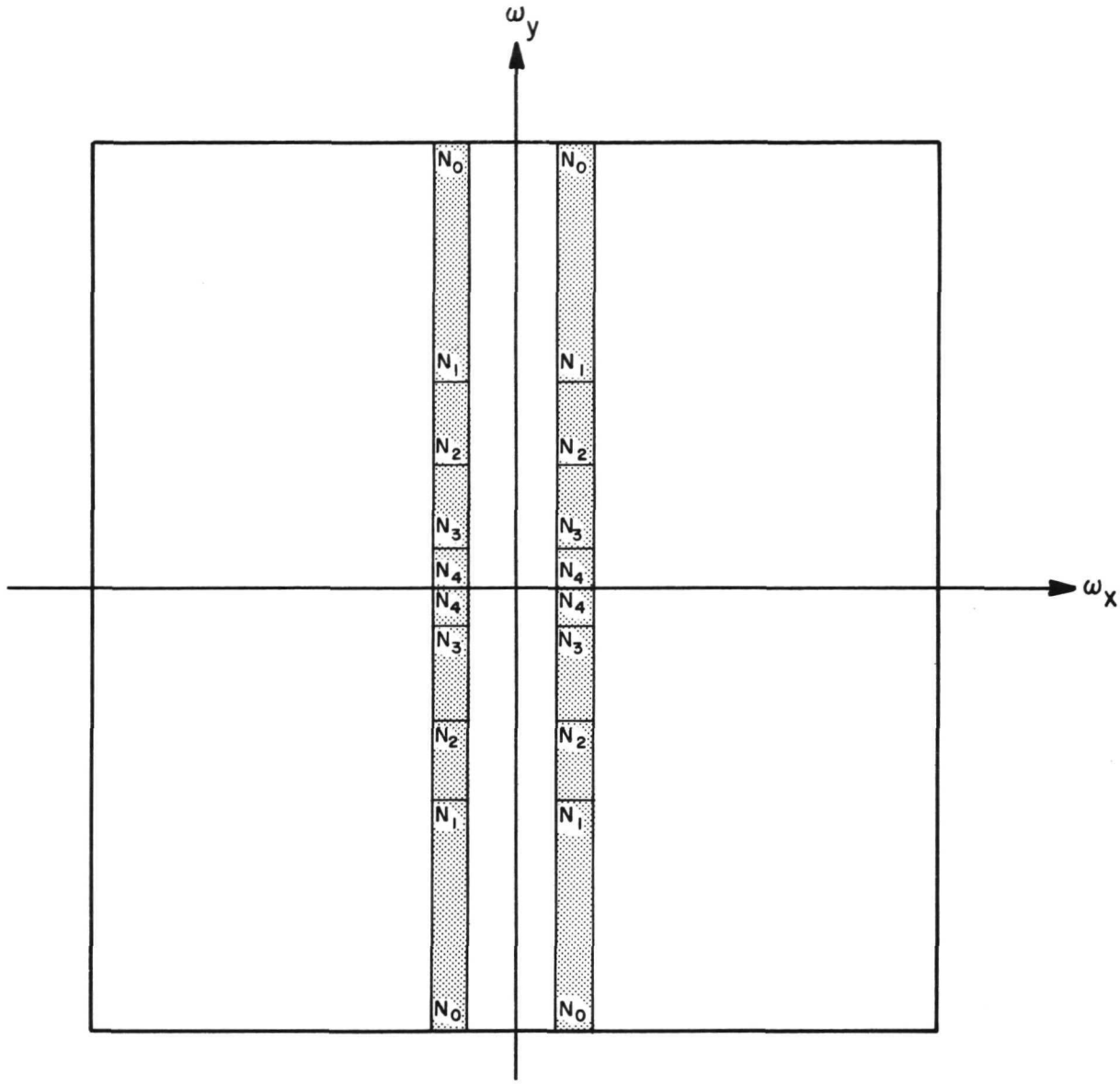

Figure 18 Four-step binary spatial filter used on the frequency representation of the noisy picture subset shown in Figure 17b.
Level N_1 corresponds to Fig. 17c and Fig. 17g.
Level N_2 corresponds to Fig. 17d and Fig. 17h.
Level N_3 corresponds to Fig. 17e and Fig. 17i.

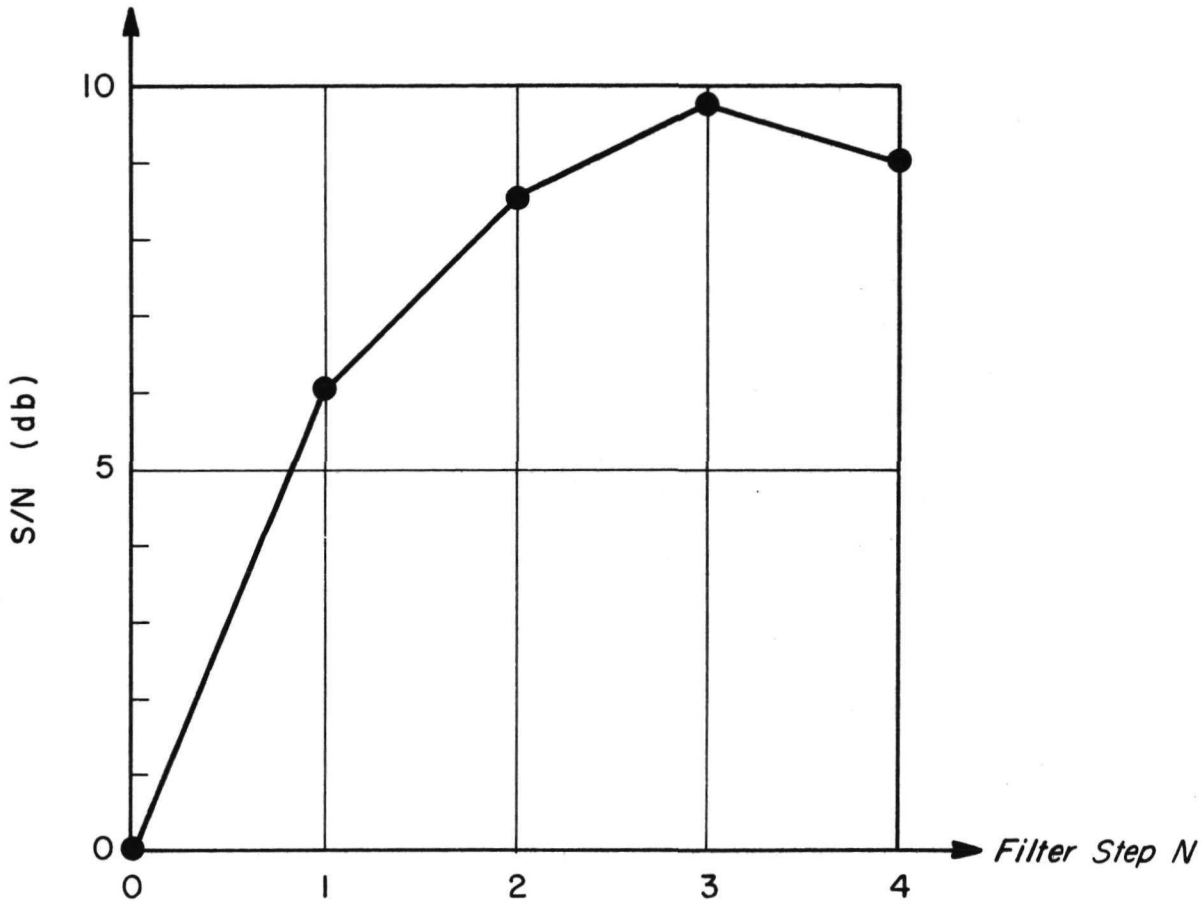

Figure 19 Signal-to-noise ratio values calculated for Figures 17b through 17e.

7831

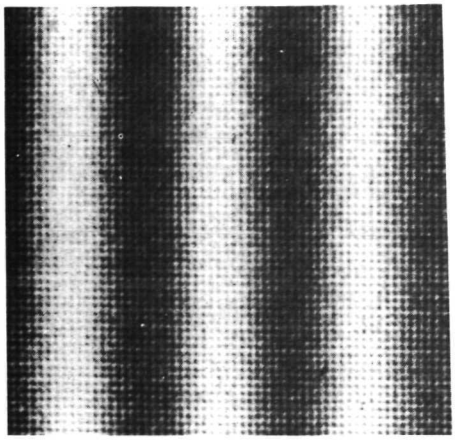

a. 64 x 64 original bar pattern window extracted from the original 512 x 512 array.

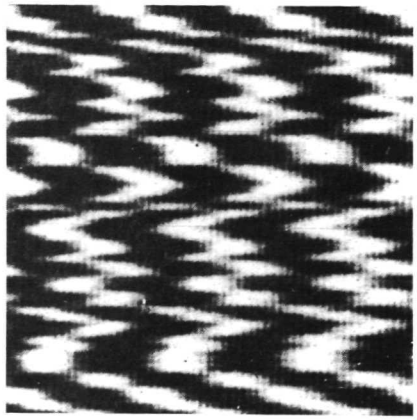

b. Herringbone noise.

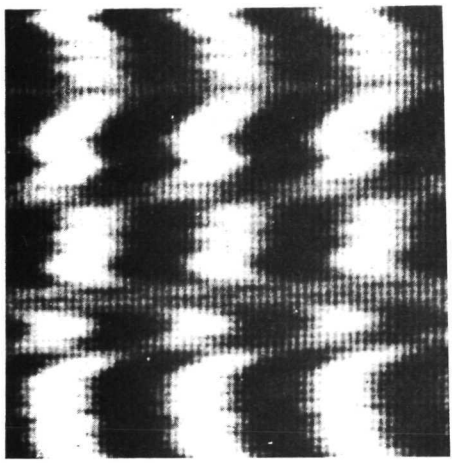

c. Bar pattern of Fig. 20. a. with herringbone noise 20. b. added.

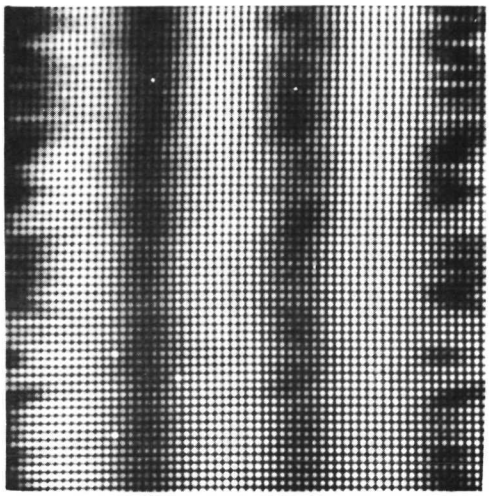

d. Results of filtering (c) in its two-dimensional spatial representation. For an explanation of the border artifacts see the footnote on page 7.

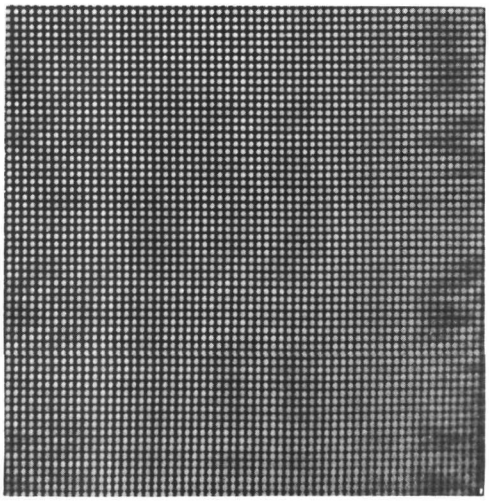

e. Residues left in the reconstructed picture after filtering.

Figure 20 Filtering herringbone noise patterns generated by a random phased sinusoid of 3.32 cpf from a sinusoidal bar battern having the same frequency.

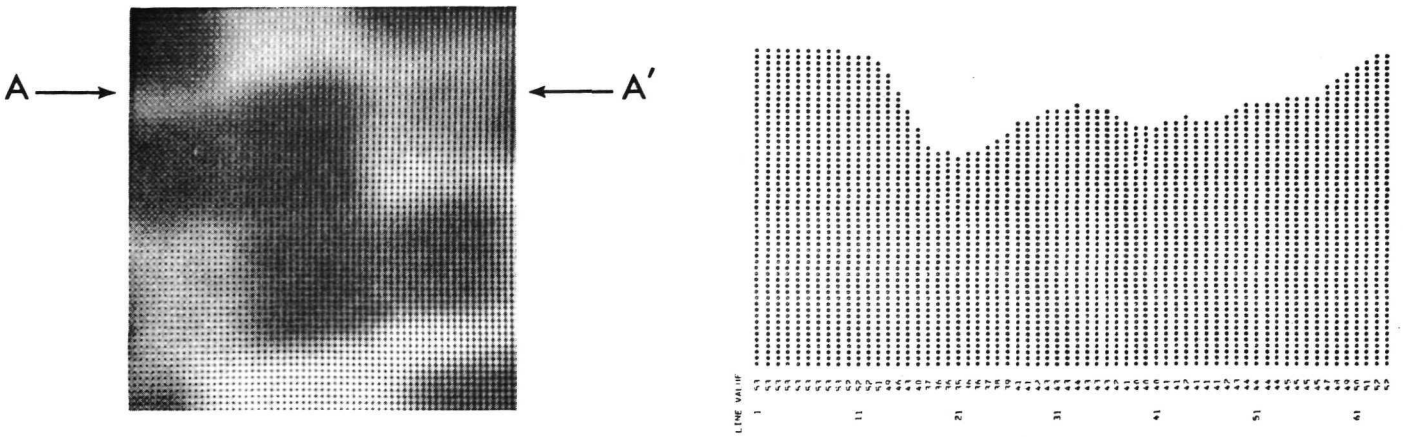

a. Grey level representation of a scan line across the input subpicture shown in Figure 17. a.

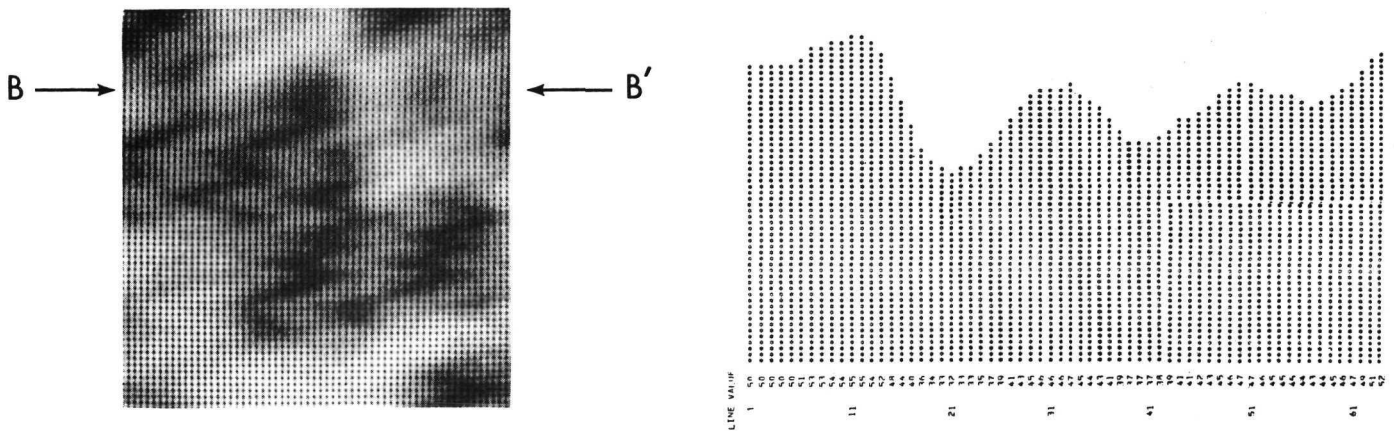

b. Grey level representation of a scan line across the subpicture shown in Figure 17. b. (noise added): local relationships are strongly perturbed.

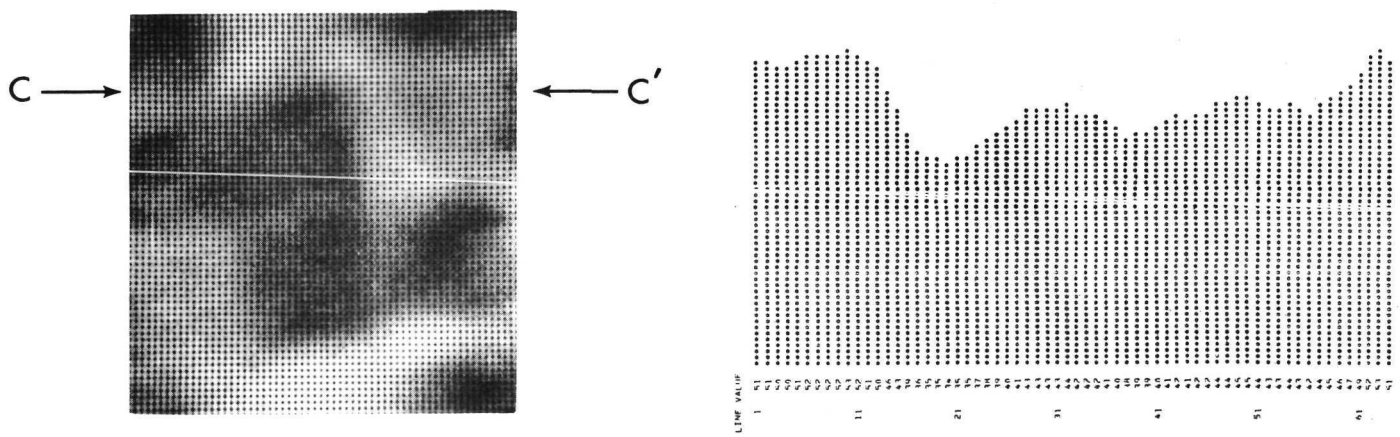

c. Grey level representation of scan line across the filtered subpicture shown in Figure 17. e.: the overall picture of Fig. 21. a. has been nearly restored.

Figure 21 Grey level representation of a typical scan line across the subpictures.

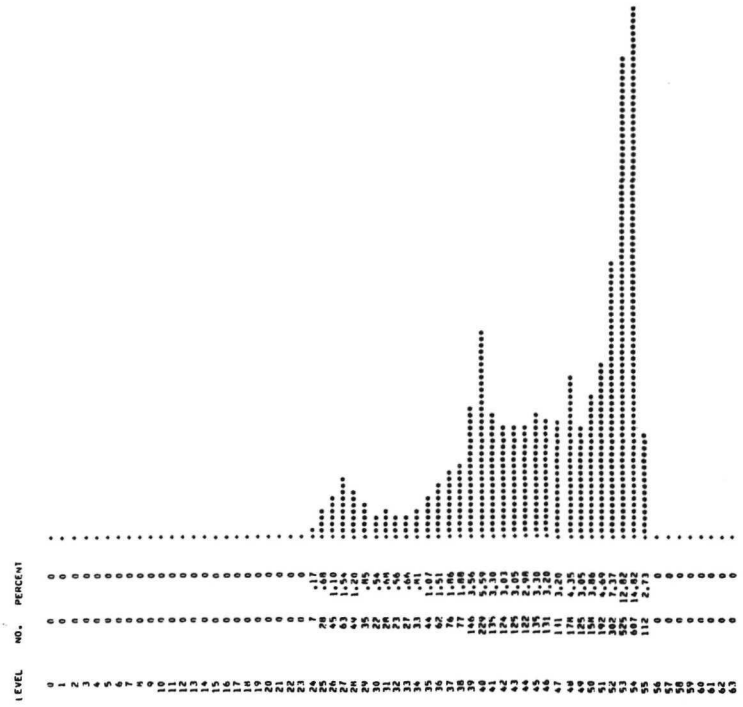

a. Grey level statistics of clean image shown in Figure 17. a.

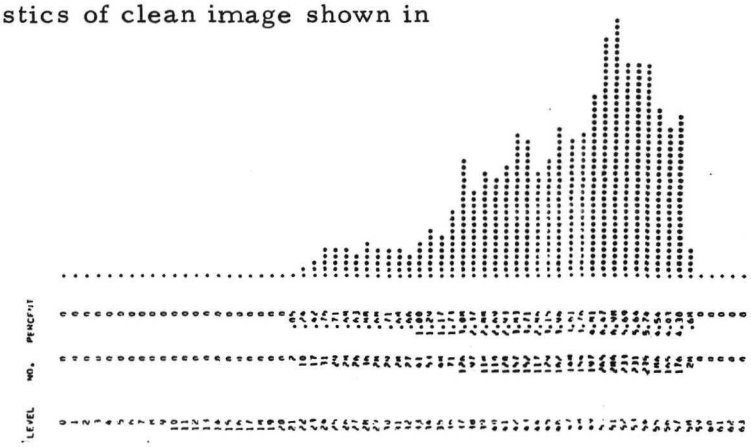

b. Grey level statistics of noisy image shown in Figure 17. b.: histogram spreads and becomes flatter.

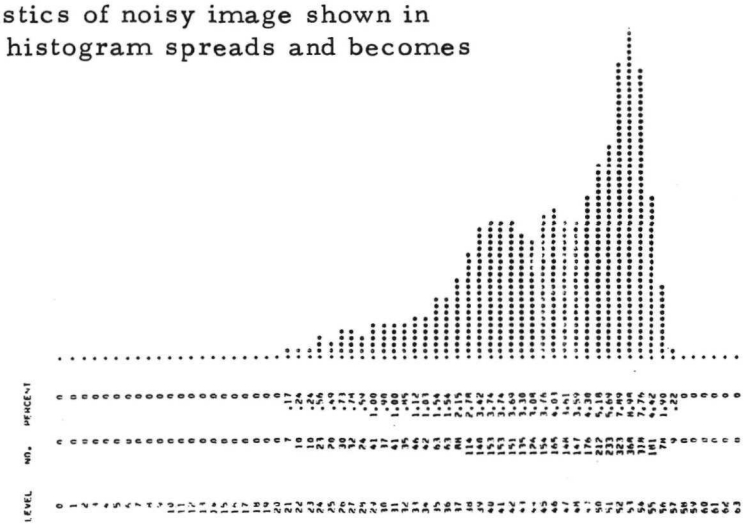

c. Grey level statistics of filtered image shown in Figure 17. e.: the overall pattern of Fig. 22. a. has been nearly restored.

Figure 22 Grey level histograms.

REFERENCES

Landgrebe, D. A., et al, 1968: LARSYSAH, A Processing System for Airborne Earth Resources Data, LARS Information Note nr. 091968, Purdue University, Lafayette, Indiana.

Mac Glamery, B. L., et al, 1969: Progress in Image Processing Techniques and Equipment, Final Report, ARPA Contract F08608-68-C-0017, Visibility Laboratory, San Diego, California.

Merritt, E. S., et al, 1969: Management, Processing and Dissemination of Sensory Data for the Earth Resources Technology Satellite, Technical Report 11, Contract NAS 5-10343.

Palgen, J. J. O., 1970: Applications of Optical Data Processing for Improving ERTS Data, Technical Report 16, Vol. 1, Contract NAS 5-10343, Allied Research Associates, Inc., Concord, Massachusetts.

Palgen, J. J. O., 1971: "Traitement Numerique de l'Information Recueillie par Satellites: les Bruits Pictoriaux," Proc. Symposium Internation "Espace et Communication" Editions Chiron, Paris.

Silverman, H. F., 1971: An Optimizing Fourier Domain Compaction Method for ERTS Data, IBM Report RC 3277, Yorktown Heights, New York.

Enochson, Loren D., Robert K. Otnes, 1968: Programming and Analysis for Digital Time Series Data. Shock and Vibration Center, Naval Research Laboratory, Washington, D.C.